Journal of Peptide Science
J. Peptide Sci. **7**: 66–79 (2002)
DOI: 10.1002/psc.370

Structural Motifs in the Maturation Process of Peptide Hormones. The Somatostatin Precursor. I. A CD Conformational Study

MARIO SIMONETTI AND CARLO DI BELLO*

Department of Chemical Process Engineering, University of Padova, 35131 Padova, Italy

Received 25 September 2001
Revised 29 October 2001

Abstract: Synthetic peptides reproducing both the native domain around the dibasic cleavage site of pro-somatostatin, and mutated sequences thereof, previously assayed in site-directed mutagenesis experiments, have been studied by CD in different solvent systems, such as water, TFE/H_2O, MeCN/H_2O and aqueous SDS, in order to ascertain the ability of each solvent to stabilize secondary structural motifs. A combination of deconvolution methods and empirical calculations, that allow subtraction of the contributions due to unordered structures from the spectra, suggests that mainly two distinct families of ordered conformers containing α-helix and/or structurally different β-turns are present in solution, the relative stability of the different conformers depending on the nature of the solvent. The presence of β-turns is in line with a previous NMR study in DMSO and DMSO/H_2O. Comparison of the CD spectra in aqueous SDS of peptides undergoing processing with a sequence not processed *in vivo* shows that only the latter possesses a stable and detectable α-helix population. This observation suggests that the structuration involving β-turns but no α-helix, which was observed by CD both in SDS and organic solvent/H_2O mixtures at high water contents, might be of biological significance. The similarity of this structuration to molecular models obtained from NMR data in DMSO and DMSO/H_2O is discussed.

Keywords: CD spectroscopy; peptide conformation; prohormone; pro-somatostatin; secondary structures; β-turns

INTRODUCTION

In mammals two peptide hormones, somatostatin-14 (S-14) and somatostatin-28 (S-28), inhibit the release of growth hormone, insulin and glucagon [1] and appear to be endogenous antiproliferative agents for a large variety of cells [2,3]. These two active peptides possess a common inactive precursor, pro-somatostatin (pro-S), encoded by a single gene [4], and are differently localized within the cells. Since the common precursor pro-S undergoes tissue specific processing to yield the active hormones S-14 and/or S-28, maturation of pro-S constitutes a very useful model in the study of the formation of multiple hormone products by differential processing of a single polyfunctional precursor [5]. Even though both the presence of different processing

Abbreviations: Abbreviations used for amino acids and peptides follow the Recommendations of the IUPAC-IUB Commission of Biochemical Nomenclature (*Eur. J. Biochem.* 1984; **138**: 9–37). The following additional abbreviations are used throughout text: MeCN, acetonitrile; CD, circular dichroism; CCA, Convex Constraint Analysis; DMSO, dimethylsulphoxide; NMR, nuclear magnetic resonance; NOE, nuclear Overhauser effect; OS, ordered structure; pro-OT/Np, precursor for ocytocin and neurophysin; pro-S, precursor of somatostatin; RMD, restrained molecular dynamics; S-14, somatostatin-14; S-28, somatostatin-28; SDS, sodium dodecylsulphate; T_A, Woody's class A dichroic pattern; T_C, Woody's class C dichroic pattern; TFE, 2,2,2-trifluoroethanol; US, unordered structure.

*Correspondence to: C. Di Bello, Department of Chemical Process Engineering, University of Padova, via Marzolo 9, 35131 Padova, Italy; e-mail: carlo.dibello@unipd.it

enzymes in the cells and the specific targeting of the precursor to different secretory pathways can explain the specific processing observed in mammals [6,7], the processing step in both hypothetical mechanisms consists of a limited proteolysis of the precursor at the basic pairs Arg^{-2}-Lys^{-1}, to give S-14, or at the single Arg^{-15} residue, to give S-28.

In the maturation of hormones and secretory peptides, the processing step is thought to involve a specific recognition machinery discerning sequence and/or structure specific determinants encoded in the precursor [4,8]. However, several experimental observations indicate that cleavage is not influenced only by the primary structure of the precursor, suggesting the existence of a more complex pathway, possibly involving some kind of structural organization of the regions surrounding the cleavage site. These factors would influence the rate of cleavage and, in some cases, determine whether the site will be cleaved or not [9], thus explaining why not all potential cleavage sites of the precursors of several hormones and other secretory peptides are processed *in vivo* [10]. The influence of the structural organization of peptide segments flanking the cleavage site has been confirmed in the case of the ocytocin/neurophysin precursor (pro-OT/Np) by a combination of spectroscopic and computer modelling techniques on a set of synthetic peptides reproducing the processing site of the pro-hormone. In particular, NMR, CD and FTIR absorption data have indicated a possible turn-helix arrangement around the processing site [11–16].

In the specific case of pro-S, site-directed mutagenesis experiments were performed in order to study the effect of a modification of the predicted secondary structure around the cleavage sites [17,18]. Modifications, such as the substitution of Ala for Pro in position −5 (Pro^{-5}; Table 1), affecting the possibility of forming β-turn structures in the immediate vicinity of the S-14 cleavage site, drastically decreased pro-S processing [17]. Other modifications included the substitution of Pro^{-5} with Gly and the replacement of the β-turn-promoting sequence Pro-Arg-Glu-Arg, corresponding to the [−5; −2] domain of pro-S, with the Ser-Ser-Asn-Arg sequence [18], which was shown to form a β-turn in 2SNS-nuclease by x-ray diffraction [19]. Interestingly, these two latter modifications did not completely abolish the cleavage at the dibasic site but affected both the relative proportions of the generated hormones and precursor processing efficiency. Accordingly, a series of five peptides, corresponding to the native domain of the pro-S and to the mutated sequences studied in the above site-directed mutagenesis experiments, was synthesized (Table 1) and studied by NMR in DMSO and DMSO/H_2O and computational methods in our laboratory [20]. These experiments indicated for both the native sequence (Som-Wtb) and the two peptides reproducing the modifications not affecting the S-14 secretion (Som-II and Som-III), the occurrence of one β-turn in each of the two regions flanking the cleavage site, i.e. [−6; −3] and [2; 5]. On the contrary, in the analogue containing the substitution $Ala^{-5} \rightarrow Pro^{-5}$ (Som-I), which abolishes cleavage at the dibasic site *in vivo*,

Table 1 Pro-S Peptides: Sequences, Cleavage and Structuration

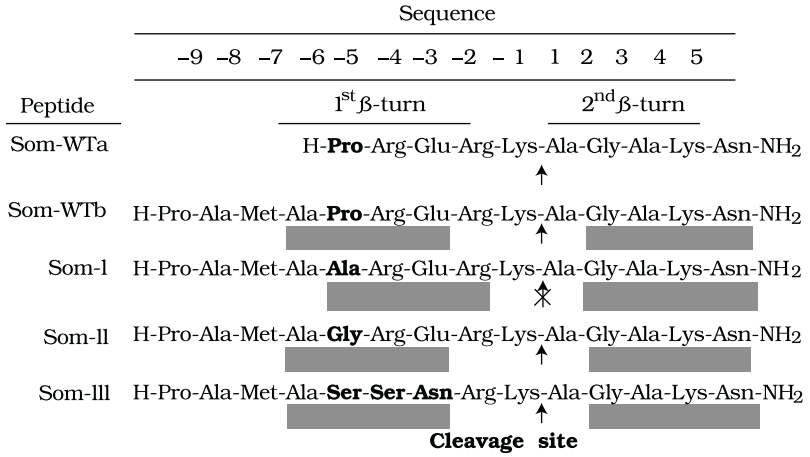

the first β-turn is shifted by one residue toward the cleavage site, thereby involving the Ala^{-5}-Arg^{-2} segment.

Even though NMR represents the most useful technique for peptide conformational analysis in solution, the NMR data should be interpreted with caution. This technique operates within a time-scale of seconds to hundredths of seconds and, as a consequence, conformational interconversions not requiring peptide bond rotations will give averaged NMR parameters that are of little value in terms of interpretation of a single conformation [21]. On the other hand, CD and FTIR absorption techniques operate on much faster scales (on the order of 10^{-15} s) [21], and hence are particularly sensitive to conformational changes. Therefore, it is not surprising that ordered conformations not seen by NMR may be detected by CD and/or FTIR absorption. Unfortunately, strong limitations arise when one tries to compare the results obtained by these different techniques. This is due to the fact that solvents may play a key role in specifically promoting one of the different conformations that can be assumed by the peptide backbone [22]; moreover, solvents commonly used by one technique quite often cannot be used by the others. In this respect, typical examples are represented by TFE, a solvent able to promote α-helical structuration of the polypeptide chain even in segments that present a different secondary organization in other solvents [22], and DMSO, a solvent extensively used for NMR that cannot be used in CD. In spite of these drawbacks, CD and FTIR absorption techniques represent very useful tools in the conformational analysis of short peptides in solution since they complete the information obtained by NMR [15,16].

In this paper a detailed analysis by CD methods of the pro-S sequences listed in Table 1 in different solvent systems such as water, TFE/H_2O, MeCN/H_2O and aqueous SDS is presented. This CD work is part of a systematic conformational study devoted to the detection of the structural motifs possessing biological relevance. The analysis of the spectra makes use of Convex Constraint Analysis (CCA) [23]. This general method is based on a set of constraints, that are able to deconvolute CD spectra into their components and related conformational weights, and on the Lincomb method [24], an algorithm based on a fit with a set of reference spectra representing known secondary structures.

MATERIALS AND METHODS

Peptide Synthesis

All peptides (Table 1) were synthesized by solid-phase methods, purified and characterized according to procedures described elsewhere [20].

CD Measurements

CD spectra were obtained at room temperature (~25 °C) using a Jasco model J-710 automatic recording circular dichrograph. Cylindrical fused quartz cells with pathlengths of 0.1 cm were employed. Before and after each series of experiments, solvent baselines were recorded under the same conditions. CD measurements were considered only when the two baselines overlapped. The solvent baseline was subtracted, and spectra were normalized in units of mean residue ellipticity (peptide molecular weight/number of amino acids) $[\theta]_R$ (deg $\times$ cm^2 $\times$ $dmol^{-1}$). Spectra subtraction, normalization and smoothing were managed by means of a personal computer with a Jasco CD data manipulation J-700 software (vers. 1.10.000) for Windows, vs. 3.1. The CD instrument was standardized with D-10-camphorsulphonic acid and epiandrosterone. In all experiments using organic solvent/H_2O mixtures, the maximum organic solvent content was 95/5, v/v, with the exception of Som-I in MeCN/H_2O where the composition was 92.3/7.7, v/v. Peptide samples were prepared by dissolving known quantities of the different peptides in a minimum amount of water, to which phosphate buffer, SDS solution, TFE or MeCN were added. Peptide concentrations, determined by mass and by peptide content (peptide-hydrolysate amino acid analysis, Waters Pico Tag System), ranged from 7.25×10^{-5} to 1.02×10^{-4} M.

Deconvolution of CD Spectra

The data base employed in the Convex Constraint Analysis (CCA) algorithm [23] used for the deconvolution of the CD spectra contained 29 different CD spectra, 5 obtained from proteins and 24 from peptides. The five proteins considered were: myoglobin, parvalbumin, adenylate kinase, insulin and lactate dehydrogenase; the corresponding CD data were taken from a review article by Yang *et al.* [25] As for peptides, together with the CD spectra of the pro-S fragments examined in the present study, the data base also includes the CD spectra of the

following pro-Ot/Np sequences: XXIV, XXV, XXIII, [Pro^7]-XXIII, [1–20], XXIX, XXXI [12]. All spectra were measured in TFE/H_2O and MeCN/H_2O at the highest organic solvent content. For peptide Som-Wta, only the spectrum in TFE/H_2O was considered. CD data on XXIV, XXV, XXIII, [Pro^7]-XXIII, [1–20] are reported in [15].

Empirical Estimation of CD Pattern

The empirical estimation of CD patterns associated to ordered populations were performed according to the method developed for pro-Ot/Np peptides [15]. This method makes use of the Lincomb program [24] employing the sets of curves obtained from CCA algorithm, and includes the following steps. (i) Calculation by the Lincomb algorithm of the concentration c_i of the conformer corresponding to each of the individual patterns of the curve set obtained from CCA application to the CD spectra in TFE/H_2O and MeCN/H_2O, at the highest organic solvent content. (ii) Repetition of the latter operation for all spectra in aqueous/organic media over the water concentrations examined. (iii) Correction of the c_i values according to a linear relation between the mean residue ellipticity at 192 nm, $[\theta]_{192}$, and the amount of ordered conformers obtained directly from the Lincomb algorithm. In this operation only the values calculated from the spectra at high organic solvent content were considered (i.e. in the solvent composition range where linearity between $[\theta]_{192}$ and Lincomb data was found). (iv) Calculation of the concentration of unordered conformers (c_{us}) at each water concentration from c_i corrected values. (v) Calculation of the pattern ascribable to the contribution of all the ordered conformers existing in solution (g_{os}) by introducing the c_{us} values in the relation:

$$g_{os}(\lambda) \approx \frac{f(\lambda) - c_{us} g_{aq}(\lambda)}{1 - c_{us}} \quad (1)$$

where $f(\lambda)$ and $g_{aq}(\lambda)$ are the experimental CD spectra at a given organic solvent concentration and in bulk water, respectively. It is assumed that $g_{aq}(\lambda)$ represents the CD pattern of unordered conformers (g_{us}). The pattern ascribable to the ordered conformer only existing at high concentration of organic solvent ($g_{os,A}$) was instead calculated by the relation:

$$g_{os,A}(\lambda) \approx \frac{f(\lambda)_{\%1} - f(\lambda)_{\%2} - [(c_{us})_{\%1} - (c_{us})_{\%2}] g_{us}(\lambda)}{(c_{us})_{\%2} - (c_{us})_{\%1}} \quad (2)$$

where %1 and %2 refer to two different water concentrations.

Examples of the $f(\lambda)_{\%1} - f(\lambda)_{\%2}$ curves introduced into Eqn (2) are the following: for Som-Wtb, the spectra in 91.9% (i) and 83.8% (ii) TFE from the spectrum in 95%; for Som-Wtb, the spectrum in 92.2% MeCN (iii) from the spectrum in 95%; for Som-I, the spectra in 83.8% (iv) and 73.1% (v) TFE from the spectrum in 95%, and the spectra in 86.6% (vi) MeCN from the spectrum in 92.3%. The sets employed with the Lincomb method [24] were *set2* for Som-Wtb, and *set4* for Som-I.

RESULTS

Measurements in Water, TFE, MeCN and SDS Solutions

Figure 1 reports the CD spectra of peptides Som-Wta, Som-Wtb, Som-I, Som-II and Som-III in 20 mM sodium phosphate buffer at pH 7, TFE, MeCN and 40 mM SDS at pH 2, 7 and 12. All spectra in water are characterized by a negative maximum below 200 nm, diagnostic of unordered conformations. On the contrary, the observation in TFE, MeCN and SDS of a positive signal below 200 nm and of a redshift in the negative band indicates the presence in solution of a conformational equilibrium between unordered structures and folded conformations. Moreover, in the case of Som-Wta, Som-Wtb, Som-I and Som-III no isodichroic point in the different spectra was observed, suggesting the existence of different conformational equilibria in TFE, MeCN and SDS. Therefore, it can be postulated that different populations of folded molecules characterized by divergent stabilities in the various solvents are present. The differences observed in SDS between spectra at different pH indicate that the ability of the surfactant to stabilize the folded conformations is affected by the charge status of the ionizable side-chains of the Lys, Arg and Glu residues.

Water Titrations of the TFE and MeCN Solutions

Since the folded populations may possess different stabilities in water, as demonstrated in the case of pro-Ot/Np fragments [15], CD spectra in TFE and MeCN were recorded at increasing water concentrations in order to pin-point the composition of the aqueous/organic mixture in which one ordered conformer is favoured with respect to the others. In the titration with water of Som-Wtb in TFE (Figure 2), the spectra recorded at TFE >80% showed a single isodichroic point around 202 nm; a second

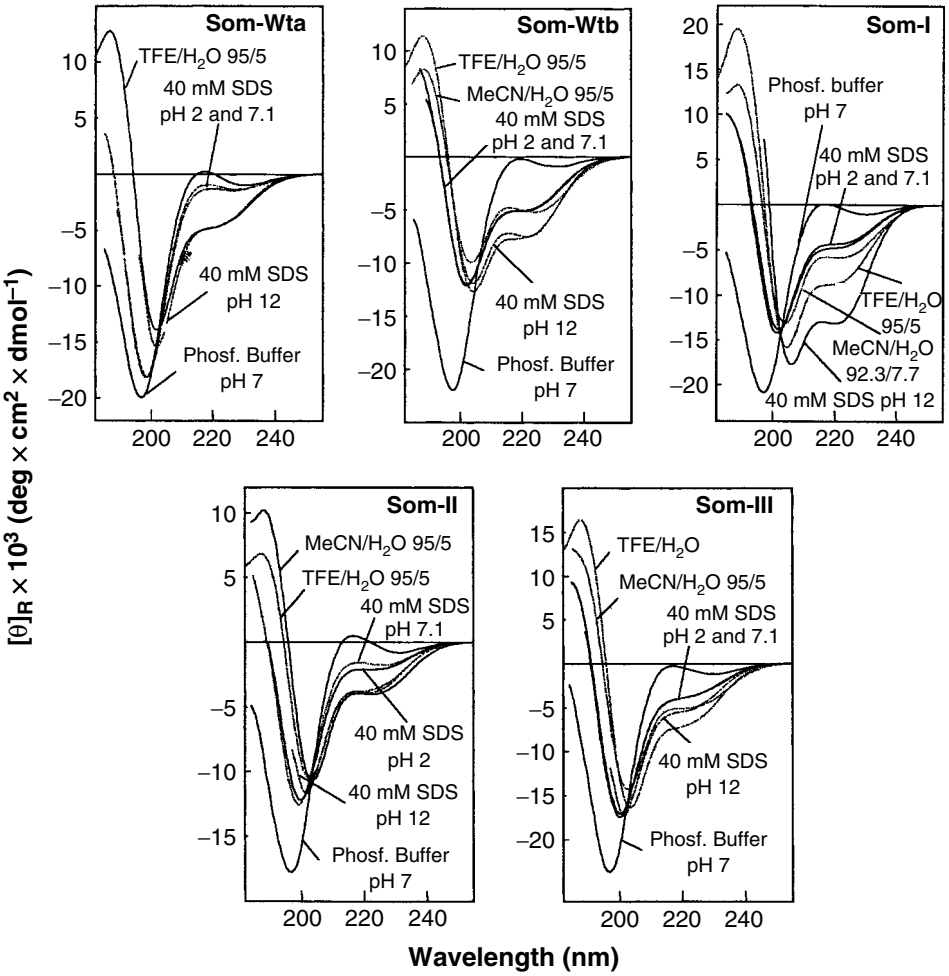

Figure 1 CD spectra of Som-Wta, Som-Wtb, Som-I, Som-II and Som-III in 20 mM sodium phosphate buffer pH 7, in 40 mM SDS solution at pH 7.1 (sodium phosphate buffer), at pH 2 (0.01 M HCl), and at pH 12 (0.01 M NaOH); and in TFE/H_2O (95/5, v/v) and MeCN/H_2O (95/5 or 92.3/7.7, v/v). mixtures.

isodichroic point at 206 nm was observed only at lower TFE content. Similar results were obtained also in the case of MeCN (Figure 2). Since it is well known that spectra identifying a single isodichroic point are representative of mixtures whose composition differs in the content of only two conformers, the observation of two distinct isodichroic points suggests the possible existence of a conformational equilibrium involving two different populations of folded chains, that are called A and B, together with unordered conformers called US (Figure 3). The ordered conformer A is stable at high organic solvent content (95%–80%); at higher water content (>20%) A is practically absent, and a conformational equilibrium is established only between the unordered population (US) and the ordered conformer B.

Similar results, characterized by two distinct isodichroic points, were obtained in the titration with water of Som-Wta in TFE (Figure 2), and of Som-I (Figure 2), Som-II and Som-III in TFE and MeCN (Figure 4). Therefore these peptides should be subjected to the conformational equilibria shown in Figure 3.

Deconvolution of CD Spectra

In the deconvolution of the CD spectra of pro-S fragments with the CCA algorithm [23] a data base similar to the one (MS 2) employed with pro-Ot/Np peptides was used [15]. This data base consisted mainly of spectra of pro-OT/Np (20 spectra) and pro-S (2 spectra) peptides, but also contained the spectra of five proteins. In the present case the original data base was modified by replacing some

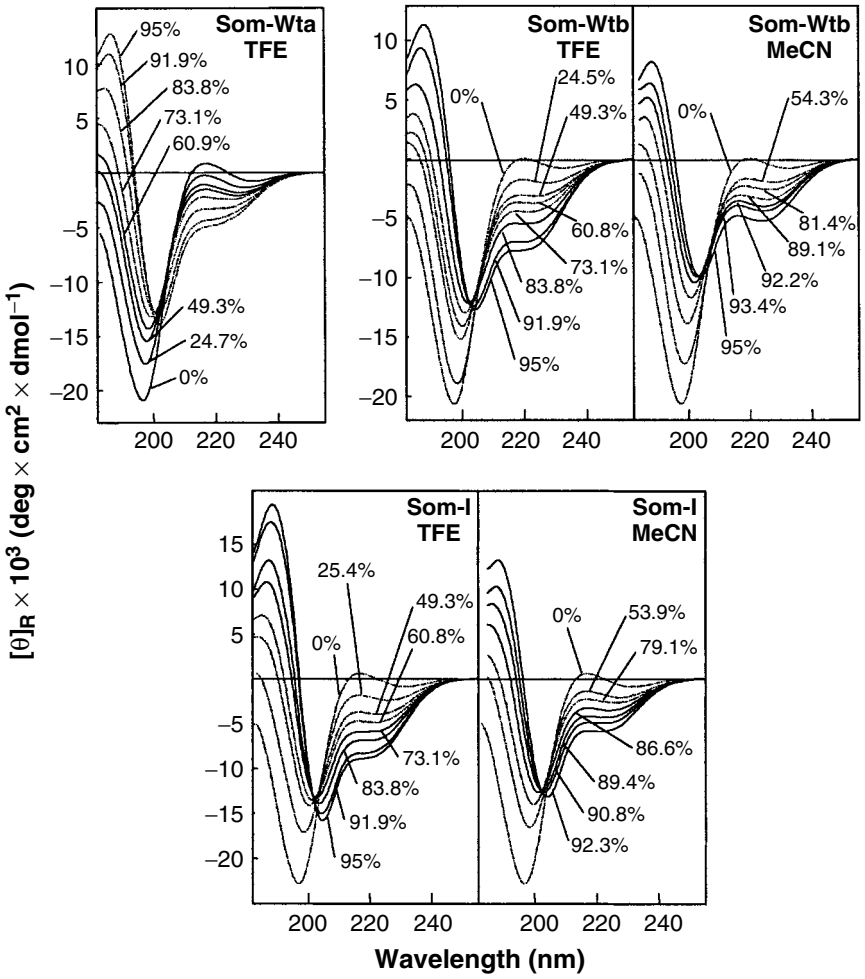

Figure 2 CD spectra of Som-Wta, Som-Wtb and Som-I at various TFE or MeCN concentrations.

spectra of pro-Ot/Np peptides with those of pro-S fragments. In this way the spectra included in the new data base resulted as follow: 5 proteins, 14 pro-Ot/Np peptides and 9 pro-S peptides. The data base has been modified in order to produce a better model for pro-S peptides. The application of the CCA algorithm with a deconvolution factor $P = 5$ to the spectrum of Som-Wtb in TFE gave the set of curves reported in Figure 5. This set (*set1*) is similar to the one obtained in the deconvolution of the spectra of pro-Ot/Np fragments [15]. As in the latter case the set presents a curve attributed to α-helix (curve A), and two patterns attributed to Woody class A (curve T_A) and class C curve (curve T_C). The typical profile of the Woody class B curve shows a first negative band at $\lambda > 200$ nm, a second positive band at 200–210 nm, and a negative signal at $\lambda < 190$ nm. In Woody class A, a blue-shifted variant of the class B curve, the first negative band is located at 210–220 nm, the second positive band at 195–200 nm, and the negative signal at $\lambda < 190$ nm [26,27]. Finally, the remaining two patterns are assigned to unordered structures (curve US) and to additional contributions (curve X_{US}). As for pro-Ot/Np fragments, this latter is probably due to unordered structures [15].

A different set of curves (*set2*) was obtained in the deconvolution of the spectra of Som-Wtb in MeCN (Figure 5). *Set2* differs from *set1* in the curves ascribable to Woody class A and class C curve (T_A and T_C), and in those assignable to unordered structures (US and X_{US}). Indeed, while the curves A of both sets nearly overlap, *set2* possesses T_A and T_C patterns with red-shifted and weaker π-π^* bands with respect to *set1*. The differences in the T_A curves appear more significant. Differences in the π-π^* bands are also seen in the US and X_{US} patterns: indeed, in *set2* the US pattern exhibits a weaker

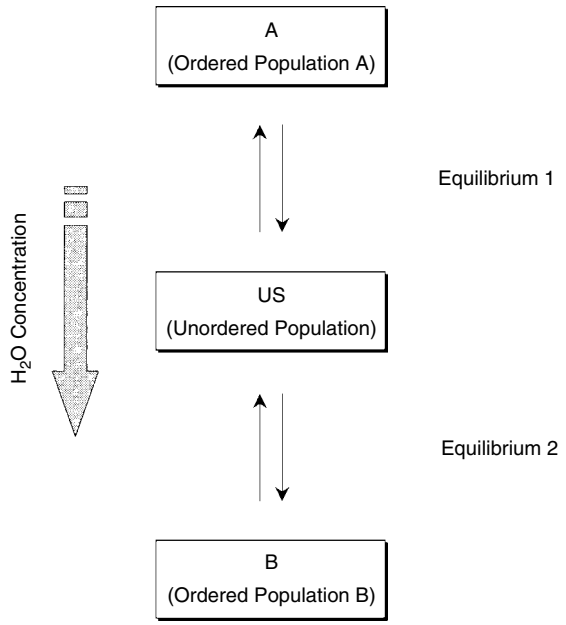

Figure 3 Schematic representation of the conformational equilibria hypothesized in TFE/H_2O and MeCN/H_2O solutions.

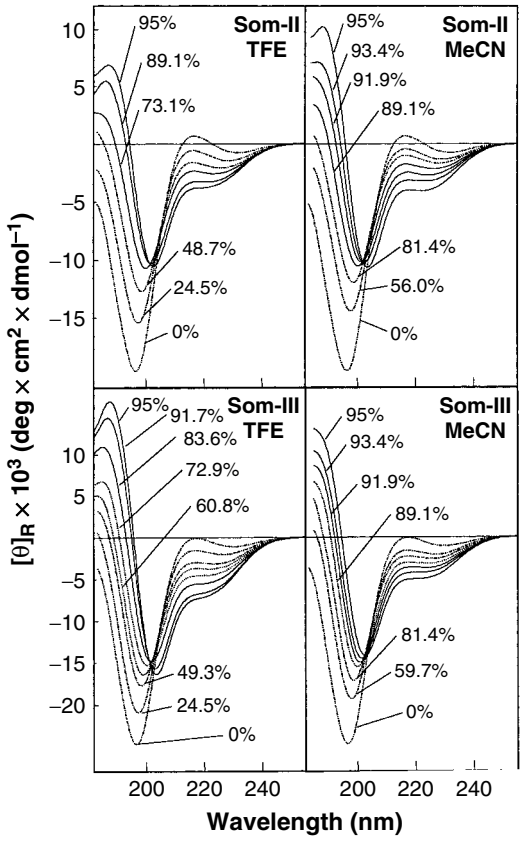

Figure 4 CD spectra of Som-II and Som-III at various TFE or MeCN concentrations.

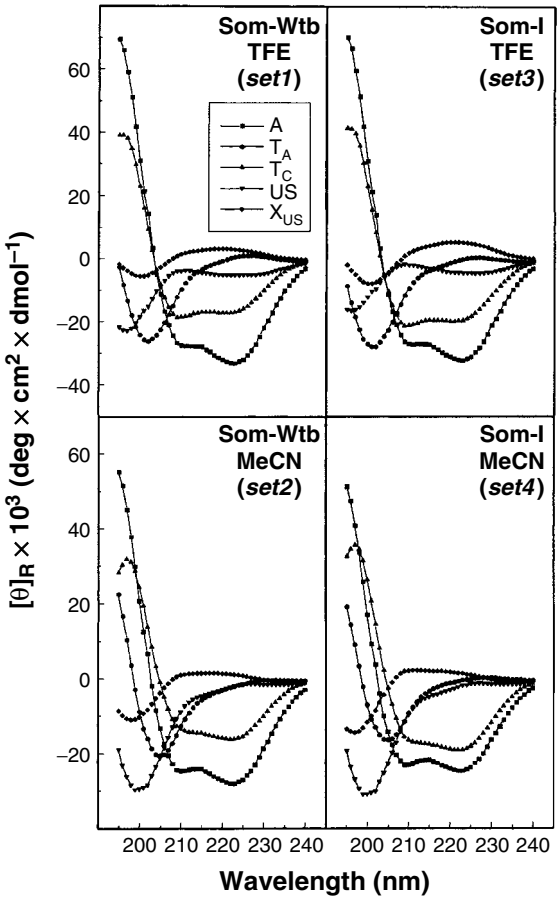

Figure 5 Analysis of the spectra of Som-Wtb and Som-I in TFE and MeCN using the CCA deconvolution algorithm. The data base is constituted by the spectra of some pro-Ot and pro-Som peptides together with those of five proteins. A, T_A and T_C refer to: α-helix, Woody class A and C patterns, respectively. US and X_{US} refers to unordered structures.

and red-shifted π-π^* band, while in X_{US} this band is more intense and blue-shifted. Two additional sets of curves (*set3* and *set4*) were obtained from Som-I in TFE and MeCN, respectively (Figure 5). The differences between these new sets were similar to those previously described for *set1* and *set2*: for example, *set4* shows T_A and T_c patterns with red-shifted π-π^* bands with respect to *set3*. Finally, application of CCA to the spectra of Som-II and Som-III in TFE and MeCN, gives the following sets of curves: *set3* (Som-II), *set4* (Som-III).

In order to verify the reliability of the above deconvolution results, each 5-curve set derived from the application of CCA program was employed in a conformational analysis of the spectra recorded during the water titrations with the Lincomb

program [24]. The results of this analysis on peptide Som-Wtb are shown in Table 2 and Figure 6. In the case of curve *set2*, the assignment of the unordered structure content to the sum of the component US and X_{US} caused overlapping of the curves relative to $\%OS/\%OS_\infty$ and $\Delta[\theta]/\Delta[\theta]_\infty$ against water content (Figure 6). On the contrary, no overlapping is observed in the case of curve *set1*, thereby indicating the limited reliability of this latter curve set. $\%OS/\%OS_\infty$ represents the ratio between the percent of ordered structures at a single intermediate point with respect to the starting point, i.e. at the maximum organic solvent content, whereas $\Delta[\theta]/\Delta[\theta]_\infty$ is the ratio between the variations at a given wavelength of $[\theta]_R$ during the titration and the maximum variation between the spectra in TFE, or MeCN, and that in water. Similar results were obtained for Som-I in TFE and MeCN (Figure 6). These observations are in agreement with the results obtained from CD analysis of pro-Ot/Np peptides [15]. Also in that case an overlap of the curves relative to $\%OS/\%OS_\infty$ and $\Delta[\theta]/\Delta[\theta]_\infty$ against water content was observed only if the unordered structure content was assigned to the sum of the component US and X_{US}, and the set of curves with T_A and T_C patterns characterized by red-shifted π-π^* bands was considered.

The results of application of the Lincomb program to the spectra measured during the water titration of the other peptides are available in the web address www.dpci.unipd.it/DipPagesIt/Biotec2.html.

Figure 7 shows the patterns calculated for Som-Wtb by introducing in Eqn (1) and (2) the c_i values obtained in the Lincomb analysis, employing *set2*. Application of Eqn (1) to the spectra at TFE concentrations <73.1% gave the spectra ascribable to the population B of conformers and generated patterns close to Woody's class B, characterized by an intense negative n-π^* band (Figure 7; patterns

Table 2 Application of the Lincomb Program Employing *set1* (a) and *set2* (b) in the Spectra Obtained in the H_2O Titration of the Solution of Som-Wtb in TFE and MeCN

	%											
H_2O	A		T_A		T_C		US		X_{US}		Deviation	
%	a	b	a	b	a	b	a	b	a	b	a	b
						TFE						
5.0	11.5	17.8	30.0	0.0	11.1	12.0	39.6	43.3	7.9	26.9	0.1	0.2
	–	0.0	–	5.2	–	36.5	–	53.3	–	5.0	–	18.7
8.1	–	13.8	–	0.0	–	13.7	–	44.1	–	28.4	–	1.0
	–	0.0	–	2.1	–	33.5	–	53.0	–	11.4	–	14.3
16.2	4.3	5.3	22.9	0.0	11.2	17.9	47.4	45.0	14.2	31.8	0.5	6.9
	–	0.0	–	0.0	–	25.9	–	48.9	–	25.2	–	8.9
26.9	–	0.0	–	0.0	–	19.8	–	47.1	–	33.1	–	11.9
39.2	0.0	0.0	21.8	0.0	8.5	15.2	52.5	46.7	17.3	38.0	2.4	17.1
50.7	–	0.0	–	0.0	–	11.7	–	46.6	–	41.7	–	21.2
75.5	0.0	0.0	26.7	0.0	0.0	3.2	58.4	50.9	15.0	45.9	30.9	41.1
100.0	0.0	0.0	25.1	0.0	0.0	0.0	57.9	48.2	17.0	51.8	188.4	74.3
						MeCN						
5.0	14.1	17.1	18.0	0.4	0.0	4.3	32.3	23.5	35.6	54.8	3.5	2.8
6.6	–	11.9	–	0.0	–	7.1	–	25.0	–	56.1	–	1.9
7.8	8.0	8.4	15.8	0.0	2.1	9.0	38.3	28.0	35.8	54.6	2.1	3.1
10.9	–	3.1	–	0.0	–	12.3	–	33.2	–	51.5	–	5.9
18.6	0.0	0.0	18.4	0.0	4.8	10.9	47.7	38.2	29.1	50.9	3.3	11.5
45.7	0.0	0.0	24.3	0.0	0.0	4.9	53.4	45.8	22.3	49.4	13.4	26.7
100.0	0.0	0.0	25.1	0.0	0.0	0.0	57.9	48.2	17.0	51.8	188.4	74.3

A, T_A and T_C refer to α-helix, to Woody class A and C patterns, respectively. US and X_{US} refer to unordered conformations.

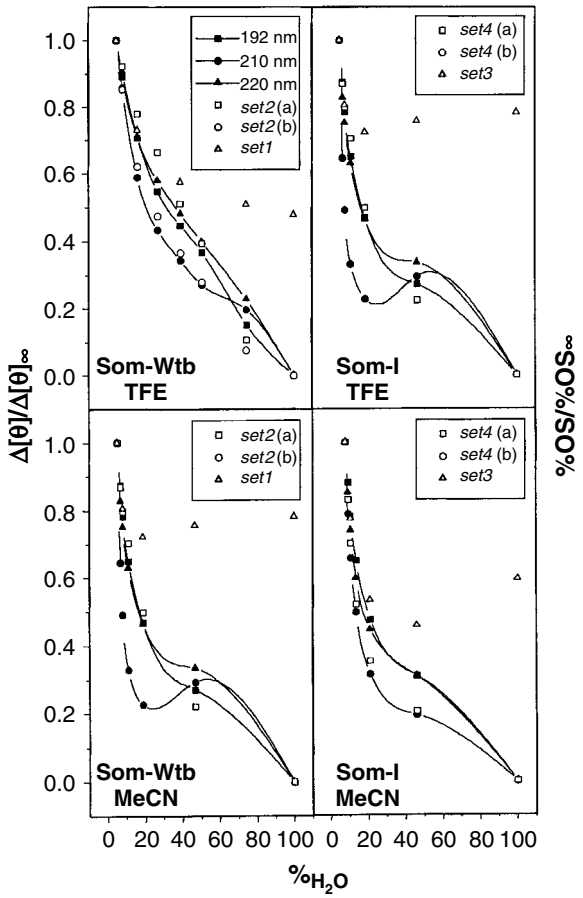

Figure 6 Plots of $\%OS/\%OS_{\infty}$ and of $\Delta[\theta]/\Delta[\theta]_{\infty}$ against water concentration derived from H_2O titrations of the solutions of Som-Wtb and Som-I in TFE and MeCN. *Set2* (a) and (b) for Som-Wtb, and *set4* (a) and (b) for Som-I, refer to different calculations by the Lincomb method [24], with *sets* 2 and 4 as reported in Table 2 and B (www.dpci.unipd.it/DipPagesIt/Biotec2.html), respectively.

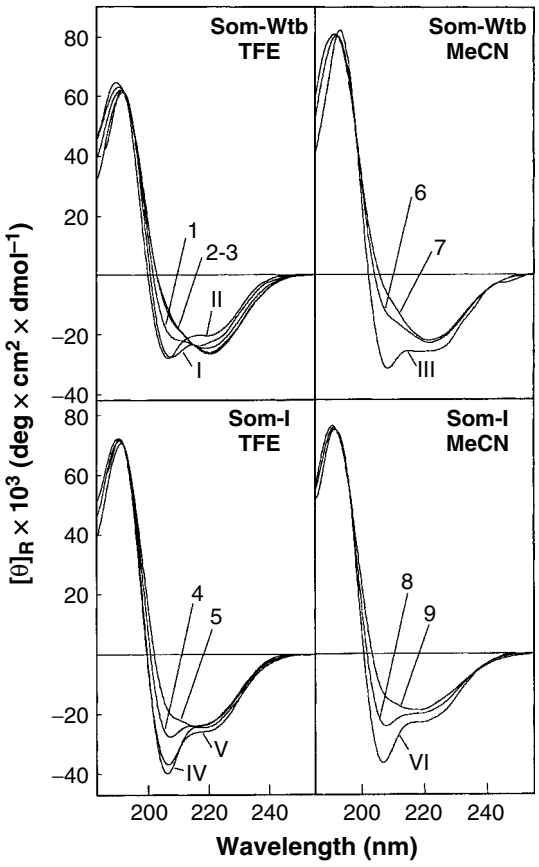

Figure 7 Estimation of CD patterns associated to the ordered populations of Som-Wtb and Som-I in TFE and MeCN. Calculations were performed by inserting c_i values derived from Lincomb method [24] in Eqn (1) (curves 1–9) and (2) (curves I–VI). Equation (1) was applied to the spectra at the following organic solvent contents: 95% (curves 1, 4, 6); 92.3% (curve 8); 49.3%–89.1% (curves 2, 3, 5, 7 and 9); the latter gave the patterns associated to the B family of ordered conformers. Curves I–VI refer to the application of Eqn (2) to the subtractions indicated in the Materials and Methods section as follows:curve I (i), curve II (ii), curve III (iii), curve IV (iv), curve V (v), curve VI (iv). Equation (2) gave the patterns associated to the A family of ordered conformers.

2 and 3). However, they differ from a pure class B pattern since a not negligible shoulder in the π-π^* region is present. Application of Eqn (2) to the two different curves obtained by subtracting the spectra in 91.9% and 83.8% TFE from the spectrum in 95% TFE gave the spectra ascribable to the population A of conformers and generated patterns characterized by both a significant negative π-π^* dichroism and a more intense n-π^* band (Figure 7; patterns I and II). The patterns I and II of Figure 7 could be attributed to the combination of a Woody class A curve with an α-helical and/or class C curve. Patterns close to Woody's class B and deriving from a combination between class A and α-helical and/or class C curves were obtained also from spectra of Som-Wtb in MeCN (Figure 7). Similar results were obtained with Som-I (Figure 7) and the other fragments Som-Wta, Som-II and Som-III.

Finally, Lincomb analysis with the more reliable *set4*, in the case of Som-Wta, Som-I, Som-II and Som-III, or *set2*, in the case of Som-Wtb, was also extended to the spectra recorded in SDS solutions. The results are reported in Table 3 along with those obtained in TFE, MeCN and water.

The data obtained for Som-Wtb indicate the existence in TFE and MeCN of a conformational

Table 3 CD Conformational Analysis of pro-S Peptides by Application of Lincomb program Employing *set4* (Som-Wta, Som-I, Som-II and Som-III) or *set2* (Som-Wtb)

Solvent	%							Deviation
	α-helix	β-turn			Unordered structures			
	A	T_A	T_C	$T_A + T_C$	US	X_{US}	$US + X_{US}$	
				Som-Wta				
TFE	13.6	5.3	4.9	10.3	37.2	39.0	76.1	2.6
	–	9.3	19.9	29.2	43.3	27.5	70.9	10.2
SDS (pH 2)	4.5	–	–	–	39.8	55.7	95.5	13.0
	–	–	5.7	5.7	42.4	51.9	94.3	7.9
SDS (pH 7)	3.7	–	–	–	37.5	58.8	96.3	13.5
	–	–	4.7	4.7	39.7	55.6	95.3	9.3
SDS (pH 12)	4.6	–	13.7	13.7	48.3	33.4	81.7	8.0
	–	0.8	19.0	19.8	50.6	29.6	80.2	9.0
H_2O	–	–	–	–	33.6	66.4	100.0	51.6
				Som-Wtb				
TFE	17.8	–	12.0	12.0	43.3	26.9	70.2	0.2
	–	5.2	36.5	41.7	53.3	5.0	58.3	18.7
MeCN	17.1	0.4	4.3	4.7	23.5	54.8	78.2	2.8
SDS (pH 2)	5.9	–	16.4	16.4	41.9	35.9	77.8	5.9
	–	–	25.3	25.3	46.2	28.6	74.8	3.9
SDS (pH 7)	7.9	–	13.6	13.6	40.8	37.8	78.6	7.9
	–	0.6	25.1	25.8	46.2	28.1	74.3	5.8
SDS (pH 12)	16.3	–	–	–	38.5	45.2	83.7	155.0
	–	–	25.6	25.6	51.1	23.3	74.4	100.1
H_2O	–	–	–	–	48.2	51.8	100.0	74.3
				Som-I				
TFE	31.1	11.1	–	11.1	40.2	17.6	57.8	0.9
MeCN	21.7	13.1	1.7	14.7	29.1	34.5	63.6	1.6
SDS (pH 2)	9.2	4.3	10.6	14.9	41.1	34.8	75.9	1.1
SDS (pH 7)	8.9	2.4	9.4	11.7	41.8	37.6	79.4	1.3
SDS (pH 12)	38.4	–	–	–	61.2	0.5	61.7	63.0
	36.5	–	2.1	2.1	61.4	–	61.4	62.1
H_2O	–	–	–	–	41.5	58.5	100.0	86.1
				Som-II				
TFE	5.7	12.6	12.6	25.2	23.4	45.7	69.1	0.5
	–	14.2	18.9	33.1	26.0	40.9	66.9	1.8
MeCN	12.1	17.0	7.0	24.0	18.7	45.3	63.9	0.8
	–	20.5	20.2	40.8	24.1	35.2	59.2	6.8
SDS (pH 2)	11.2	–	1.9	1.9	22.3	64.6	86.9	11.2
	–	3.7	13.1	16.8	28.0	55.2	83.2	2.3
SDS (pH 7)	10.1	–	0.1	0.1	20.9	68.9	89.8	10.1
	–	1.6	11.9	13.5	26.1	60.4	86.5	2.8
SDS (pH 12)	14.4	–	–	–	23.5	62.1	85.6	35.1
	–	–	18.0	18.0	31.8	50.3	82.1	12.8
H_2O	–	–	–	–	29.2	70.8	100.0	35.2

Table 3 (*Continued*)

Solvent	%							Deviation
	α-helix	β-turn			Unordered structures			
	A	T_A	T_C	$T_A + T_C$	US	X_{US}	$US + X_{US}$	
	Som-III							
TFE	22.1	9.5	2.8	12.3	47.7	17.9	65.6	0.4
	–	15.6	27.1	42.7	57.3	–	57.3	20.7
MeCN	18.4	5.7	1.8	7.6	38.0	36.1	74.1	1.4
	–	11.0	22.0	33.1	46.3	20.7	66.9	15.3
SDS (pH 2)	11.4	–	–	–	49.4	39.2	88.6	17.3
	–	–	14.2	14.2	56.0	29.9	85.8	6.4
SDS (pH 7)	12.0	–	–	–	48.0	40.1	88.0	13.8
	–	–	14.8	14.8	54.8	30.3	85.2	4.2
SDS (pH 12)	12.7	–	–	–	48.5	38.8	87.3	77.5
	–	–	16.0	16.0	55.9	28.1	84.1	51.2
H_2O	–	–	–	–	48.6	51.4	100.0	142.5

A T_A and T_C refer to α-helix, to Woody class A and C patterns, respectively. US and X_{US} refer to unordered conformations.

equilibrium in which the α-helix (A: 17.1%–17.8%) should be favoured with respect to the β-turns with Woody's class C dichroism (T_C: 4.3%–12.0%). In TFE, a second calculation where the α-helix was excluded ($T_A + T_C + US + X_{US}$) gave results characterized by deviations considerably higher (18.7) than those found with the first calculation that included the α-helix (0.2). On the contrary, in SDS the β-turns appear to be favoured with respect to the α-helix, which was in this case negligible or even absent. Similar results were obtained with Som-Wta. Compared with Som-Wtb, Som-I in TFE and MeCN should possess higher contents of α-helix (A: 21.7%–31.1%) and β-turns with Woody's class A dichroism (T_A: 13.1%–11.1%), while those of class C were absent or negligible. Moreover, also for Som-I the SDS brought about a destabilization of the α-helix (A: 8.9%–9.2%) and the conformational equilibrium was shifted towards the β-turns with Woody's class C dichroism (T_A: 2.4%–4.3%; T_C: 9.4%–10.6%). For Som-III the solvent effect on the conformational equilibrium was the same, but with this latter peptide the ordered conformations were less stable than for Som-I. On the contrary, with Som-II, both in organic media (TFE and MeCN) and aqueous SDS, the conformational equilibrium was characterized by a higher content of β-turns with respect to α-helix. In particular, in TFE and MeCN the β-turn dichroism was of Woody's classes A and C, while in SDS the ordered conformations were less stable and characterized mainly by β-turns with Woody's class C dichroism.

CONCLUSIONS

Experimental evidence supports the hypothesis that turns and larger loops may play an important role in the proteolytic events leading to the maturation of secretory peptides from their larger precursors [13,28,29]. The importance of turns and loops as structural motifs of biological relevance could be a consequence of the fact that they have been shown to be almost invariably located on the external surface of proteins and to possess a greater degree of flexibility and local mobility, compared with more rigid structures such as α-helices and β-sheets, thus favouring both accessibility and adaptability to proteolytic enzymes. Synthetic model peptides reproducing both native and selectively modified sequences of inactive precursors have been synthesized, tested as substrates, and subjected to conformational analysis by different spectroscopic techniques in order to determine how structure may play a functional role in enzyme recognition, substrate binding and, consequently, prohormone processing. An example is represented by peptides reproducing sequences around the Lys^{11}-Arg^{12} doublet of the pro-OT/Np precursor. In this case the combined use of NMR measurements, in DMSO

and/or DMSO/H_2O, and RMD techniques, and those of CD and FTIR absorption in different solvents, has enabled the formulation of a molecular model for the preferred solution conformation of the entire processing domain, in which the peptide chain around the processing site is arranged as {β-turn}-{Lys^{11}-Arg^{12}}-{α-helix} [11–16,30].

However, as the application of NMR to short linear and usually flexible peptides gives observed spectral parameters which represent weighted averages between the interconverting conformers, the molecular models based on these data cannot be safely correlated to well defined structural motifs, that might be relevant to the biological process [21]. On the contrary, the faster time scale of both CD and FTIR absorption makes these techniques very useful in obtaining information on each conformer existing in solution and on the shifts in the conformational equilibria brought about by the different solvents. Unfortunately, at variance with NMR, it is almost impossible to obtain specific information regarding individual residues from CD and FTIR absorption data. Therefore, in the study of the complex relation between structure and properties of peptide substrates it is very important to complete the conformational analysis based on NMR data with the characterization by CD and FTIR absorption of the different conformer populations that a peptide may assume as a function of its molecular environment.

The present paper reports a CD study on a set of synthetic peptides, modelled on the processing site of pro-S, in several membrane-mimetic media, including TFE, MeCN and aqueous SDS at various pHs. In particular, the results obtained in the titration with water of the organic solutions indicated the existence of two distinct populations of ordered conformers. Moreover, application of the CCA software [23] to the measurements in TFE and MeCN led to the deconvolution of the CD spectra in a set of five curves containing the α-helix pattern, and those ascribable to class A and C, according to Woody's classification [26]. The set of five reference curves derived from the application of CCA permitted the conformational analysis of the CD spectra in the different solvents by using the Lincomb software [24]. The data so obtained (Table 3) indicated that in all solvents one or more populations of conformers involving β-turns were present for the five peptides; in TFE and MeCN a second population containing α-helical tracts was also present. On the contrary, in aqueous SDS the α-helix was present only in Som-I, while in the other peptides it was absent or negligible. In organic mixtures, increasing amounts of water resulted in the destabilization first of the α-helix, and then of the β-turns. Therefore, one can conclude that different conformational equilibria are present in organic mixtures and in aqueous SDS; the α-helix was more stable in the former media, and β-turns in aqueous SDS.

These data fit well with those of a parallel NMR study in DMSO and DMSO/H_2O on the same peptides [20], in which an equilibrium between a folded conformation, involving two distinct β-turns, and a random structure was suggested. Unfortunately, the characteristics of the media used for NMR do not allow CD measurements under the same experimental conditions. However, as proposed for pro-Ot/Np peptides [15], it can be postulated that, due to its strong proton acceptor properties, DMSO would preferentially stabilize the T_C conformation that was found in aqueous SDS, and in TFE and MeCN only in the presence of high water concentrations. Thus, the model based on the NOE effects observed in DMSO and DMSO/H_2O would be amenable to this specific ordered population.

From a biological point of view, it is significant to compare the results obtained from the peptides corresponding to the sequences undergoing processing *in vivo*, i.e. Som-Wta, Som-Wtb, Som-II and Som-III, with those obtained from Som-I, which is the only sequence not processed [18]. Comparison among results in organic media indicates a higher stability of the α-helix for Som-I, with respect to the other fragments. However, since for Som-III this difference is rather small, the results of the conformational analysis in organic solvents are not sufficient to explain the different behaviour of the pro-S sequences in the processing *in vivo*. On the contrary, the data in aqueous SDS do show a significant difference: in this solvent, indeed, a population of α-helix is stable and detectable in the case of Som-I, while for the other peptides no α-helical conformers are detected. Therefore, the structuration observed both in SDS, organic solvent/H_2O mixtures at high water contents and, possibly, DMSO and DMSO/H_2O, mainly characterized by the T_C conformation, should be of biological significance. On the other hand, NMR data in DMSO and DMSO/H_2O permitted the formulation of molecular models for all the pro-S peptides. Interestingly, the same model, involving one β-turn in each of the two regions [−6; −3] and [2; 5] flanking the cleavage site (Table 1), was common to all sequences processed *in vivo*, namely Som-Wta, Som-Wtb, Som-II and Som-III [18,20]. On the contrary, in the model for Som-I,

the only sequence not processed, the first β-turn is shifted by one residue toward the cleavage site, thus including one of the amino acids (Arg^{-2}) of the dibasic pairs [18,20]. In conclusion, the hypothesis that the pro-S involves a T_C conformation is in good agreement with the biological data. Moreover, both the inclusion of Arg^{-2} in the first β-turn, as shown by the NMR derived model, and the stabilization of an α-helical conformation, as shown by CD analysis, may explain the lack of processing of the Som-I sequence. These conclusions demonstrate the complementarity between the information derived from NMR and that derived from the CD technique. Finally, despite the enormous challenge represented by the precise definition of the structure of a substrate at the receptor site, the presence of several families of ordered conformers is in line with current theories that hold that the catalytic effect of the receptor microenvironment might be determinant in shifting the equilibrium toward the active conformation [31].

REFERENCES

1. Brown M, Rivier J, Vale W. Somatostatin-28: selective action on the pancreatic β-cell and brain. *Endocrinology* 1983; **108**: 2391–2393.
2. Morcau JP, De Feudis FV. Pharmacological studies of somatostatin and somatostatin-analogs: therapeutic advances and perspectives. *Life Sci.* 1987; **40**: 419–437.
3. Schally AV. Oncological application of somatostatin analogues. *Cancer Res.* 1988; **48**: 6977–6985.
4. Argos P, Taylor WL, Minth CD, Dixon JE. Nucleotide and amino acid sequence comparisons of prepro-somatostatins. *J. Biol. Chem.* 1983; **258**: 8788–8793.
5. Brakch N, Rholam M, Nault C, Boileau G, Cohen P. Differential processing of hormone precursor: independent production of somatostatins 14 and 28 in transfected neuroblastoma 2A cells. *FEBS Lett.* 1991; **282**: 363–367.
6. Gluschankof P, Gomez S, Morel A, Cohen P. Enzymes that process somatostatin precursors. *J. Biol. Chem.* 1987; **262**: 9615–9620.
7. Bourdais J, Pierotti AR, Boussetta H, Barre N, Devilliers G, Cohen P. Isolation and functional properties of an arginine-selective endoprotease from rat intestinal mucosa. *J. Biol. Chem.* 1991; **266**: 23386–23391.
8. Lepage-Lezin A, Joseph-Bravo P, Devilliers G, Benedetti L, Launay JM, Gomez S, Cohen P. Pro-somatostatin is processed in the Golgi apparatus of rat neural cells. *J. Biol. Chem.* 1991; **266**: 1679–1688.
9. Geisow MJ, Smyth DG. In *The Enzymology of Post-translational Modifications of Proteins*, Freedman RB, Howkins HC (eds). Academic Press: London, 1980; 259–287.
10. Gluschankof P, Cohen P. Proteolytic enzymes in the post-translational processing of polypeptide hormone precursors. *Neurochem. Res.* 1987; **12**: 951–958.
11. Créminon C, Rholam M, Boussetta H, Marrakchi N, Cohen P. Synthetic peptide substrates as models to study a pro-ocytocin/neurophysin converting enzyme. *J. Chromatogr.* 1988; **440**: 439–448.
12. Brakch N, Boussetta H, Rholam M, Cohen P. Processing endoprotease recognizes a structural feature at the cleavage site of peptide prohormones. The proocytocin/neurophysin model. *J. Biol. Chem.* 1989; **264**: 15912–15916.
13. Paolillo L, Simonetti M, Brakch N, D'Auria G, Saviano M, Dettin M, Rholam M, Scatturin A, Di Bello C, Cohen P. Evidence for the presence of a secondary structure at the dibasic processing site of prohormone: the pro-ocytocin model. *EMBO J.* 1992; **11**: 2399–2405.
14. Di Bello C, Simonetti M, Dettin M, Paolillo L, D'Auria G, Falcigno L, Saviano M, Scatturin A, Vertuani G, Cohen P. Conformational studies on synthetic peptides reproducing the dibasic processing site of pro-ocytocin-neurophysin. *J. Pept. Sci.* 1995; **1**: 251–265.
15. Simonetti M, Falcigno L, Paolillo L, Di Bello C. CD conformational studies on synthetic peptides encompassing the processing domain of the ocytocin/neurophysin precursor. *Biopolymers* 1997; **41**: 461–479.
16. Simonetti M, Di Bello C. New Fourier transform infrared based computational method for peptide secondary structure determination. II. Application to study of peptide fragments reproducing processing site of ocytocin-neurophysin precursor. *Biospectroscopy* 2000; **62**: 109–121.
17. Gomez S, Boileau G, Zollinger L, Nault C, Rholam M, Cohen P. Site-specific mutagenesis identifies amino acid residues critical in prohormone processing. *EMBO J.* 1989; **8**: 2911–2916.
18. Brakch N, Boileau G, Simonetti M, Nault C, Joseph-Bravo P, Rholam M, Cohen P. Pro-somatostatin processing in Neuro2A cells. Role of β-turn structure in the vicinity of the Arg-Lys cleavage site. *Eur. J. Biochem.* 1993; **216**: 39–47.
19. Cotton FA, Hazen EE, Legg MJ. Staphylococcal nuclease: proposed mechanism of action based on structure of enzyme-thymidine 3′,5′-biphosphate-calcium ion complex at 1.5-Å resolution. *Proc. Natl. Acad. Sci. USA* 1979; **76**: 2551–2555.
20. Falcigno L, Fraternali F, Manduca DM, D'Auria G, Simonetti M, Di Bello C, Paolillo L. A conformational study in solution of pro-somatostatin fragments by NMR and computational methods. *J. Pept. Sci.* 1998; **4**: 305–318.
21. Rose GD, Gierasch LM, Smith JA. Turns in peptides and proteins. *Adv. Protein Chem.* 1985; **37**: 1–109.

22. Mutter M, Hersperger R. Peptides as conformational switch: medium-induced conformational transitions of designed peptides. *Angew. Chem. Int. Ed. Engl.* 1990; **29**: 185–187.
23. Perczel A, Hollósi M, Tusnády G, Fasman GD. Convex constraint analysis: a natural deconvolution of circular dichroism curves of proteins. *Protein Eng.* 1991; **4**: 669–679.
24. Perczel A, Park K, Fasman GD. Analysis of the circular dichroism spectrum of proteins using the convex constraint algorithm: a practical guide. *Anal. Biochem.* 1992; **203**: 83–93.
25. Yang JT, Wu CS, Martinez HM. Calculation of protein conformation from circular dichroism. *Methods Enzymol.* 1986; **130**: 208–269.
26. Woody RW. In *Peptides, Polypeptides and Proteins*, Blout ER, Bovey FA, Goodman M, Lotan N (eds). Wiley: New York, 1974; 338–350.
27. Hollósi M, Köver KE, Holly S, Radics L, Fasman GD. β-turns in bridged proline-containing cyclic peptide models. *Biopolymers* 1987; **26**: 1555–1572.
28. Rholam M, Nicolas P, Cohen P. Precursors for peptide hormones share common secondary structures forming features at the proteolytic processing site. *FEBS Lett.* 1986; **207**: 1–6.
29. Bek E, Berry R. Prohormonal cleavage sites are associated with ω-loops. *Biochemistry* 1990; **29**: 178–183.
30. Falcigno L, Paolillo L, D'Auria G, Saviano M, Simonetti M, Di Bello C. NMR conformational studies on a synthetic peptide reproducing the [1–20] processing domain of the pro-ocytocin-neurophysin precursor. *Biopolymers* 1995; **39**: 837–848.
31. Schwyzer R. Peptide–membrane interactions and a new principle in quantitative structure–activity relationships. *Biopolymers* 1991; **31**: 785–792.

